Transient Measurements of Adsorption and Diffusion in H-ZSM-5 Membranes

Tracy Q. Gardner, Ana I. Flores, Richard D. Noble, and John L. Falconer
Dept. of Chemical Engineering, University of Colorado, Boulder, CO 80309

A transient permeation method presented here not only determines the adsorption and diffusion properties of the pores that are the transport pathways through zeolite membranes, but nondestructively estimates the effective thickness of the membrane. Transient responses of the permeate concentration to step changes in the feed were measured on two H-ZSM-5 tubular membranes and modeled assuming Maxwell-Stefan diffusion and Langmuir adsorption. The adsorption isotherms determined from these transient measurements at 298 K of N_2 and CO_2 were nearly identical to those measured by calorimetry on H-ZSM-5 powders. The CH_4 isotherm at 298 K was similar to isotherms measured by calorimetry and gravimetric techniques on Na-ZSM-5 and silicalite powders. The similarity of the isotherms indicates that transport of these light gases occurs mainly through zeolite pores. The Maxwell-Stefan diffusion coefficients $Đ_{MS}$ depended on concentration and were higher for higher feed partial pressures. Average $Đ_{MS}$ values for the two membranes were 7.5, 5 and 1.5×10^{-10} m^2/s for N_2, CH_4, and CO_2, respectively; these are in the same range and order as diffusion coefficients measured in zeolite crystals.

Introduction

Zeolites are crystalline aluminosilicates with pore sizes between 0.3 and 1.3 nm. Zeolite membranes are polycrystalline films of these materials grown on porous supports that provide mechanical stability. Because their pore sizes are of molecular dimensions and they have high chemical and thermal stability, zeolite membranes have the potential to perform many industrially important separations. They are also catalytically active and may be useful for catalytic membrane reactors.

Most zeolite membrane research has been on synthesis, characterization, and permeation behavior of films on stainless steel or alumina supports. Films of zeolite types MFI (Bai et al., 1995; Bakker et al., 1996; Bein, 1996; Davis and Lobo, 1992; den Exter et al., 1996; Gora et al., 2001; Jia et al., 1994; Kapteijn et al., 1995a,b; Matsukata et al., 1993; Noble and Falconer, 1995; Tuan et al., 1999; Xomeritakis et al., 1999; Yan et al., 1995), FER (Matsukata et al., 1996; Nishiyama et al., 1997), FAU (Bein, 1996; Kusakabe et al., 1998, 1999), LTA (Bein, 1996; Hedlund et al., 1997; Matsukata and Kikuchi, 1997), MOR (Bein, 1996; Matsukata and Kikuchi, 1997), MEL (Tuan et al., 2001), ANA (Matsukata and Kikuchi, 1997), AFI (Bein, 1996), and zeolite L (Bein, 1996) have been reported, with silicalite and ZSM-5 (both of the MFI structure type) receiving the most attention. Framework substitution, where some of the Si or Al atoms in the framework are replaced by other atoms such as boron, germanium, and iron, has improved membrane properties in some cases (Kosslick et al., 1993; Tuan et al., 2000), and boron-substituted ZSM-5 membranes showed good separation behavior at high temperatures (Tuan et al., 2000).

Zeolite membranes separate gas and liquid mixtures based on differences in the diffusion coefficients and adsorption properties of the permeating components. Diffusion through zeolite pores is assumed to follow a five-step process involving sorption onto the surface from the gas phase; transport into, through, and out of the pores; and desorption into the gas phase at the opposite side (den Exter et al., 1996). The conditions (temperature, partial pressure, molecule and crystal characteristics) determine which step will dominate the diffusion. Barrer (1990) outlined criteria for determining the importance of interfacial effects. If the crystal is thick enough (or the membrane is thick and well enough intergrown), interfacial processes are not limiting and intracrystalline diffusion dominates the transport. This is usually the case for diffusion through zeolite membranes under normal operating conditions. Fickian diffusion with a concentration-indepen-

dent diffusion coefficient does not qualitatively describe some transport phenomena observed for diffusion through zeolites. For example, when Bakker et al. (1993) fed a $H_2/n\text{-}C_4$ mixture to a silicalite-1 membrane, H_2 initially permeated faster than $n\text{-}C_4$, but its flux decreased below the $n\text{-}C_4$ flux at longer times. Fickian diffusion predicts a monotonic rise of each gas rather than a maximum in the more weakly sorbing component, suggesting that constant diffusion coefficient is qualitatively incorrect for describing multicomponent diffusion through zeolites. Zeolite pore diffusion has been modeled by applying the Darken correction factor (a coverage-dependent thermodynamic factor) to a corrected diffusion coefficient, which was then assumed to be independent of coverage (den Exter et al., 1996). This approach was applied in the Maxwell-Stefan diffusion model, where, for single component diffusion, the corrected diffusion coefficient is referred to as the Maxwell-Stefan diffusion coefficient ($Đ_{MS}$). The Maxwell-Stefan model has been extended to mixture diffusion, and it qualitatively describes the transient multicomponent diffusion through zeolites and zeolite membranes, such as the $H_2/n\text{-}C_4$ experiment performed by Bakker et al., whereas the Fickian model does not (Kapteijn et al., 1995b; Krishna and van den Broeke, 1995).

The Maxwell-Stefan model has also been applied to steady-state permeation through zeolite membranes for quantitative determination of diffusion coefficients (Kapteijn et al., 1995). Diffusion coefficients determined for membranes by this technique are of the same order of magnitude as those determined for crystals by other macroscopic techniques such as frequency response (Bulow et al., 1986), uptake measurements (Bulow et al., 1986), and chromatography (Hufton and Danner, 1993). In contrast, diffusion coefficients for zeolite crystals determined by microscopic techniques (pulsed field NMR (Caro et al., 1985; Datema et al., 1991), quasi-elastic neutron scattering (Jobic et al., 1989), molecular dynamics (Catlow et al., 1991; Goodbody et al., 1991; Maginn et al., 1993)) are up to 3 orders of magnitude higher. Invalid assumptions made in analysis of macroscopic data (Kapteijn et al., 1995), differences in the interpretation of equilibrium vs. nonequilibrium measurements (Jobic et al., 1999), and the inaccuracy of each technique when applied near its limits (Sun et al., 1996) are among the reasons suggested for these large differences. Transport techniques that measure diffusion through membranes have the advantage of only characterizing the pathways involved in transport and of providing effective diffusion coefficients that include effects of non-idealities in structure such as surface barriers and intercrystalline regions.

Sun et al. (1996) used transient measurements to determine the intracrystalline diffusion coefficients of CO_2 and $C_1\text{-}C_4$ alkanes through a single crystal of silicalite embedded in epoxy. They measured the transient response to step changes in the feed and modeled the flux assuming Fickian diffusion. Their feed pressures were between 0 and 7 kPa, so Fickian diffusion was a reasonable assumption because coverages were low enough that any dependence of D on coverage could be neglected. From their transient adsorption and desorption curves, they obtained diffusion coefficients for CO_2 and $C_1\text{-}C_4$ alkanes in the 10^{-10} m^2/s range, which is between the ranges reported in the literature for diffusion through zeolite crystals from microscopic methods (10^{-10} to 10^{-9} m^2/s) and from other macroscopic methods (10^{-12} to 10^{-11} m^2/s). Their results were closer to the spectroscopic measurements than diffusion coefficients measured previously by monitoring the transient pressure rise on the low-pressure side of a single crystal membrane. Sun et al. concluded that their diffusion coefficients were more accurate than the previous results, because they used a concentration driving force rather than a pressure driving force and because they monitored the permeating species with a mass sensitive detector rather than measuring a small pressure rise near zero pressure.

The adsorption properties of light gases and hydrocarbons in silicalite and ZSM-5 zeolite crystals have been measured by calorimetric (Dunne et al., 1996a,b), chromatographic (Hufton and Danner, 1993), gravimetric (Choudhary and Mayadevi, 1996; Sun et al., 1998), and transient pulse response (Nijhuis et al., 1999) methods. Zhu et al. (1998) used a tapered element oscillating microbalance (TEOM) to measure the adsorption properties of light alkanes in silicalite-1. Molecular simulations have also been used to calculate adsorption isotherms based on molecular level sorbent/sorbate interactions (June et al., 1992, 1990; Mentzen, 1995; Skoulidas and Sholl, 2001). The results from these techniques differ, and a range of adsorption parameters for the same zeolite type, adsorbent, and temperature conditions is reported in the literature. All these adsorption studies were on zeolite crystals (or simulated atomistic structures), and adsorption isotherms have not previously been measured for zeolite membranes. Adsorption on ZSM-5 zeolites is affected by the Si/Al ratio (Dunne et al., 1996a,b), which cannot be directly measured in a nondestructive manner for supported zeolite membranes. Adsorption coverages tend to increase with increasing Al content (Dunne et al., 1996a,b).

Generally, the Si/Al ratio reported for membranes is either that of the synthesis gel or a ratio measured for crystals synthesized simultaneously with the membrane. Measurement of adsorption parameters for a zeolite membrane by a transport technique would be advantageous, because the pathways contributing to the transport would be characterized directly, and these adsorption parameters may be different from those of zeolite crystals.

This article describes a technique for determining adsorption and diffusion parameters and film thicknesses of zeolite membranes by measuring and modeling the transient response of the permeate concentration to step changes in the feed. This technique is nondestructive and only characterizes the pathways involved in transport. Langmuir adsorption isotherms generated by this analysis for light gases on H-ZSM-5 membranes are compared to those for powders, and Maxwell-Stefan diffusion coefficients and their dependence on concentration are measured.

Experimental Methods

Membrane preparation

Porous sintered stainless steel tubes (0.65-cm ID, 2.5-cm long, Mott Metallurgical Co.) with 500-nm diameter pores were used as supports for the zeolite membranes. Nonporous stainless steel tubes (1 cm in length) were welded onto the ends of the porous supports to provide smooth surfaces for sealing the membranes into the permeation module. Alkali-

free H-ZSM-5 membranes were crystallized hydrothermally on the inside surfaces of the supports. Silica sol (Ludox AS40) was the silicon source, aluminum isopropoxide (Aldrich, 98+%) was the aluminum source, and tetrapropylammonium hydroxide (TPAOH) was the template for ZSM-5 synthesis. A clear gel with a molar composition of 438 H_2O: 19.5 SiO_2: 0.0162 Al_2O_3: 1 TPAOH was used. One end of each support tube was wrapped in Teflon tape and covered with a Teflon cap, and the tubes were filled with approximately 2 mL of synthesis gel. As the gel soaked into the porous supports, the tubes were refilled throughout the day. The supports were left to soak overnight and were refilled three more times the following day. The other end was then wrapped with Teflon tape and covered with a Teflon cap before placing the tube in a Teflon-lined autoclave. The first zeolite layer was synthesized for 22 h (M1) or 48 h (M2) at 458 K. The tubes were then rinsed with D.I. water, brushed on the inside surface to remove loose crystals, and dried for 10 min in a vacuum oven at 383 K. After synthesis of the second and third layers (48 h, 458 K), N_2 at 138 kPa was used to determine if the membranes were gas tight. If N_2 permeation was detected, another layer was added. The membranes required three layers before being impermeable to N_2 prior to calcination.

After the zeolite films were grown, the membranes were dried in a vacuum oven at 383 K overnight. The template was removed from the zeolite pores by calcination at 758 K in stagnant air. Heating and cooling rates were 0.01 K/s and 0.018 K/s, respectively, and the membranes were held at 758 K for 8 h.

Transient permeation measurements

A Wicke-Kallenbach system with helium as the carrier gas was used for the transient permeation measurements. The membranes were sealed in a stainless steel module with Viton o-rings on each nonporous end. Before each measurement, helium flowed on the feed (inside of the tube) and permeate sides of the membrane, and the module was heated to 473 K to remove adsorbed species. Both the helium feed gas and the gas to be studied flowed at 100 cm^3/min (standard temperature and pressure) to a manual switching valve that sent one inlet to a vent and the other to the membrane feed side. Initially helium flowed to the membrane and the gas of interest flowed to the vent. When the valve was switched, helium went to the vent and the test gas was fed to the membrane. Back pressure regulators on the retentate and bypass lines were adjusted so the feed pressures of the helium and the test gas were each at 120 kPa and did not change when the flows were switched. The response in the permeate concentration to this step change in the feed was monitored with a quadrupole mass spectrometer (Pfeiffer Vacuum Prisma) that monitored multiple mass peaks simultaneously. The total flow was measured with a bubble flowmeter.

To determine the system response time and any deviation from a step input change on the feed side, transient measurements were also carried out on a support without a zeolite layer since its permeance was more than 1,000 times higher than that through a zeolite membrane. Two seconds after the feed valve was switched, the signal for the test gas on the permeate side was at 98% of its steady-state value. This time included the times for the feed gas to reach the support, flow through it, and for the sweep gas to carry the permeate to the mass spectrometer.

Theory

Diffusion through zeolites is assumed to follow a five step process: (1) adsorption onto the surface; (2) migration into the micropore; (3) diffusion through the micropore; (4) migration out of the pore onto the surface; and (5) desorption from the surface (den Exter et al., 1996). Barrer (1990) determined for a wide range of temperature, coverage, permeant, and crystal thickness conditions that, for interfacial effects (steps 1, 2, 4, and 5) to play an important role in diffusion, the crystal must be 1 μm or smaller and the temperature low (90 K for permanent gases). Therefore, permeation through thicker zeolites and zeolite membranes at higher temperatures is generally assumed to be limited by intracrystalline diffusion. The generalized Maxwell-Stefan theory qualitatively describes single- and multicomponent diffusion (step 3) for gas diffusion through zeolites. The theory is based on a balance between the driving force exerted on a particular species and the friction it experiences with all other species in the mixture and with the adsorbent surface (Krishna, 1993).

Based on single file diffusion of a pure component through zeolite pores, transient surface occupancies (fraction of available adsorption sites that is occupied; $\theta = q/q_{sat}$) can be described by

$$\frac{\partial \theta}{\partial t} = \frac{\partial}{\partial z}\left(D\frac{\partial \theta}{\partial z}\right) \tag{1}$$

where D is the Fickian micropore diffusion coefficient (m^2/s). In the Maxwell-Stefan model, the diffusion coefficient is multiplied by a thermodynamic factor, called the Darken correction factor

$$D = Đ_{MS}\Gamma \tag{2}$$

$$\Gamma = \frac{q}{P}\frac{\partial P}{\partial q} \tag{3}$$

where $Đ_{MS}$ is the coverage independent Maxwell-Stefan diffusion coefficient (m^2/s), q is the coverage (mol/kg zeolite), and P is the partial pressure of the permeating component (kPa). The thermodynamic factor Γ is determined from the adsorption isotherm. For light gases on MFI-type zeolites, Langmuir single site adsorption can be assumed

$$\theta = \frac{q}{q_{sat}} = \frac{bP}{1+bP} \tag{4}$$

where q_{sat} (mol/kg zeolite) and b (kPa^{-1}) are Langmuir adsorption parameters. From this, the thermodynamic factor can be calculated as:

$$\Gamma = \frac{1}{1-\theta} \tag{5}$$

Combining Eqs. 2 and 5, yields the single component diffusion coefficient

$$D = \frac{Đ_{MS}}{1-\theta} \tag{6}$$

The boundary conditions from the Langmuir adsorption isotherm are

$$\theta_0 = \frac{q_0}{q_{sat}} = \frac{bP_0}{1+bP_o} \tag{7}$$

at the feed side ($z = 0$) and

$$\theta_\delta = \frac{q_\delta}{q_{sat}} = \frac{bP_\delta}{1+bP_\delta} \tag{8}$$

at the permeate side ($z = \delta$). The initial condition is that the membrane is empty ($\theta = 0$). Equation 1 with these boundary and initial conditions can be solved numerically to obtain the coverage profiles across the thickness of the membrane as a function of time. The molar flux through the membrane (mol/m^2 s) can then be calculated from the coverage gradient at the permeate boundary

$$J = -\rho q_{sat} D \left.\frac{\partial\theta}{\partial z}\right|_{z=\delta} \tag{9}$$

where ρ is the zeolite density (kg/m^3). This expression is used to model the transient flux measured on the permeate side of the membrane.

Integration of Eq. 1 once over z yields an expression for $d\theta/dz$ that can be applied at the permeate boundary and combined with Eq. 9 to obtain a relationship between $Đ_{MS}$, δ, and the steady state flux (J_{SS})

$$\frac{Đ_{MS}}{\delta} = \frac{J_{SS}}{\rho q_{sat} \ln\left(\frac{1+bP_0}{1+bP_\delta}\right)} \tag{10}$$

This equation can be used to calculate $Đ_{MS}$ from the steady-state flux and feed and permeate partial pressures of adsorbent when the adsorption properties and membrane thickness are known.

Complete integration of Eq. 1 applied at steady state with boundary conditions 7 and 8 yields the steady-state coverage profile

$$q(z) = q_{sat} - (q_{sat} - q_0)\left(\frac{q_{sat}-q_\delta}{q_{sat}-q_0}\right)^{z/\delta} \tag{11}$$

Figure 1 shows how the coverage profile changes with time as the membrane fills and empties; the dashed line represents the steady-state profile. Integrating Eq. 11 yields an equation

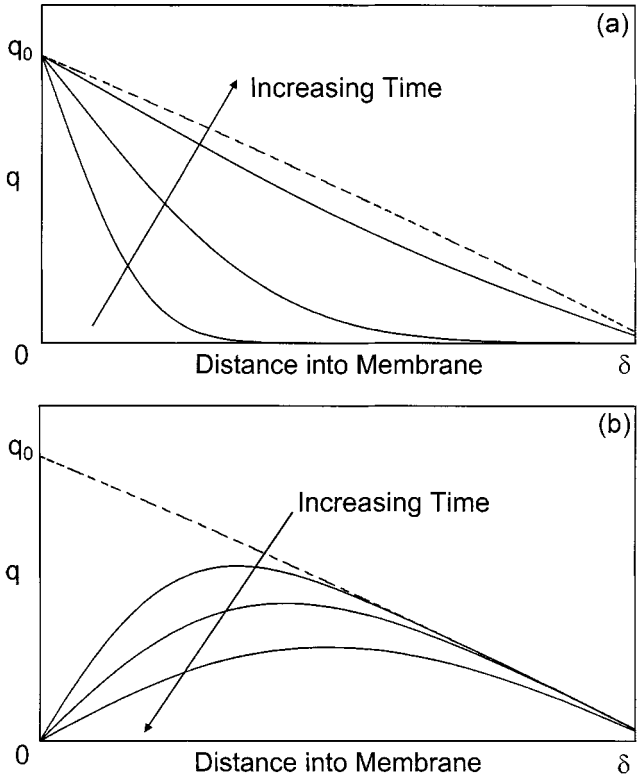

Figure 1. Coverage profile evolution across membrane with thickness δ after step change in feed to (a) feed pressure of $P_0 > 0$ kPa (membrane filling) and (b) feed pressure of $P_0 = 0$ kPa after attaining steady-state flux (membrane emptying), based on Maxwell-Stefan diffusion with Langmuir adsorption at $z = 0$ and zero coverage on the permeate side.

Dashed line = steady-state profile.

for the total number of mols in the membrane at steady state

$$Q_c = \rho A q_{sat}\delta\left(1 + \frac{\frac{q_0-q_\delta}{q_{sat}}}{\ln\left(\frac{q_{sat}-q_0}{q_{sat}-q_\delta}\right)}\right) \tag{12}$$

This equation assumes the membrane is a single crystal of cross-sectional area A and thickness δ, and the subscript c denotes that it was determined from the steady-state coverage profile.

The total number of mols in the membrane at steady state can also be determined from the transient flux. The accumulation of molecules in the membrane, per unit cross-sectional area, is equal to the flux in (J_{in}) minus the flux out (J_{out}). Integration of this difference from the step feed change ($t = 0$) until steady state ($t = t_{SS}$) and multiplying the result by the membrane area yields the total number of mols in the membrane at steady state (Q_t)

$$Q_t = A\cdot\int_0^{t_{SS}}(J_{in} - J_{out})dt \tag{13}$$

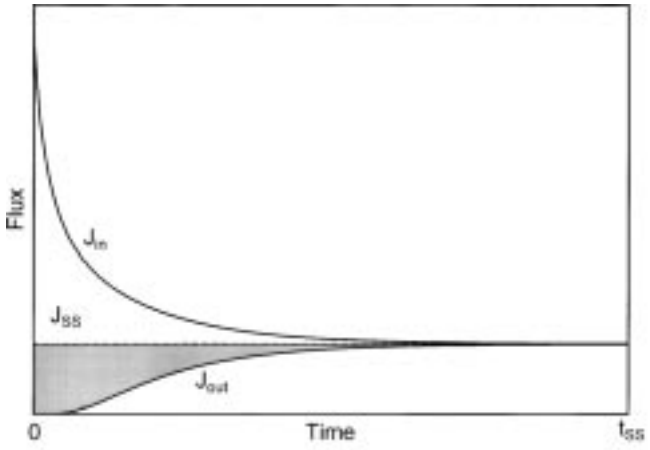

Figure 2. Flux into and out of the membrane modeled as Maxwell-Stefan diffusion.

The shaded area represents the integral from $t = 0$ to $t = t_{SS}$ of $(J_{SS} - J_{out})$.

The subscript t indicates that this measure of the total amount of mols in the membrane at steady state is determined from the transient flux. The flux out can be calculated from Eq. 9, and the flux into the membrane can be calculated from a similar equation applied at the feed side boundary

$$J_{in} = -\rho q_{sat} D \left.\frac{\partial \theta}{\partial z}\right|_{z=0} \tag{14}$$

The profiles in Figure 1 show that the coverage gradient at the feed side is high initially for a step increase in the feed concentration, and the gradient decreases as the membrane fills. This means that J_{in} is high initially and decreases to the steady-state value J_{SS}. The flux out does the opposite, starting at zero and increasing with time to J_{SS} (Figure 2).

The flux out can be measured, but the flux in cannot be accurately measured. Therefore, to calculate Q_t from measured quantities, the area under the curve between J_{in} and J_{out} was compared to the area under the curve for $(J_{SS} - J_{out})$ (gray area in Figure 2) and the following relationship was found

$$\int_0^{t_{SS}} (J_{in} - J_{out})\,dt = 3\int_0^{t_{SS}} (J_{SS} - J_{out})\,dt \tag{15}$$

Equation 15 has been proven analytically for Fickian diffusion (Gardner et al., 2002) and has been verified for Maxwell-Stefan diffusion by numerical solution of Eq. 1 for all the permeation conditions used in this study.

Adsorption Isotherms and Membrane Thicknesses

From the measured transient and steady-state fluxes, Q_t (the total mols in the membrane at steady state) can be calculated using Eq. 13 with the assumption that $(J_{in} - J_{out}) = 3\,(J_{SS} - J_{out})$ for each gas at each feed pressure. By equating Q_t to Q_c, the membrane thickness and adsorption isotherm parameters can be determined. Combining Eqs. 7, 8, 12, 13, and 15 yields

$$\rho q_{sat}\delta\left(1 - \frac{b(P_0 - P_\delta)}{(1+bP_0)\cdot(1+bP_\delta)\cdot\ln\left(\dfrac{1+bP_0}{1+bP_\delta}\right)}\right) = 3\cdot\int_0^{t_{SS}} (J_{SS} - J_{out})\,dt \tag{16}$$

where the lefthand side is calculated (Q_c) and the righthand side is measured (Q_t). By minimizing the sum of squared errors (SSE) for $(Q_c - Q_t)^2$ for a set of three or more feed conditions, the fitting parameters δ, q_{sat}, and b can be determined simultaneously. When adsorption isotherms are generated for multiple gases through multiple membranes, the number of adjustable parameters is $(2g + m)$, where g is the number of gases and m is the number of membranes—one pair of q_{sat} and b for each gas and one thickness for each membrane. As long as transients for at least three feed concentrations are measured for each gas/membrane system, the sum of squared errors can be minimized over the entire data set so all membrane thicknesses and adsorption parameters are determined simultaneously

$$SSE = \sum_g \sum_m (Q_c - Q_t)^2 \tag{17}$$

This assumes that the adsorption properties for a given gas are the same in all membranes. The two membranes used were both H-ZSM-5 prepared with the same gel composition in the same manner, so their adsorption properties should be the same. Therefore, the data for the three gases through both membranes were used together to determine the adsorption parameters and membrane thicknesses. The Solver package in Microsoft Excel minimized the sum of squared errors by varying q_{sat}, b, and δ within limits of 0.01–12 mol/kg, 0.0001–0.1 kPa^{-1}, and 30–500 μm, respectively. Solver requires a set of initial guesses for the variable parameters. Guesses close to and far from the expected parameter values were used to assure that the regression analysis did not converge to different solutions depending on the starting values. The solution was the same for all initial guesses.

Diffusion Coefficients

After the adsorption parameters and effective membrane thicknesses were known, Maxwell-Stefan diffusion coefficients were calculated from the steady-state fluxes using Eq. 10. Maxwell-Stefan diffusion with Langmuir type 1 adsorption assumes the coverage dependence of the diffusion coefficient is described by Eq. 6, where $Đ_{MS}$ is independent of coverage. Experiments and molecular simulations have shown that this assumption is not always valid (Jobic et al., 1999; Kapteijn et al., 1995b; Skoulidas and Sholl, 2001). If $Đ_{MS}$ depends on coverage, then the diffusion coefficients determined from this technique represent averaged values across the membrane.

Transient Permeation

The transient mass balance in Eq. 1 was solved numerically using the method of lines. The spatial derivatives were approximated by finite differences and the time derivative was solved using the Adams Gear ODE solver in the IMSL libraries of Microsoft Visual C++™. The membrane thickness was divided into three sections with smaller node spacing in the first section where gradients were higher and the equations were stiffer. For calculation of the area under the flux in vs. time curve ($J_{in} - J_{out}$), the node spacing in the z direction was decreased further to account for the stiffness of the equation because of the high gradients at the feed boundary. The area under this curve approached three times the area under the ($J_{SS} - J_{out}$) curve as the node spacing was reduced.

The transient fluxes were calculated from the membrane thickness, adsorption parameters, and diffusion coefficients determined from the above analysis, and the parameters were not further adjusted to fit the model to the measured transient responses. The switch from light gas to helium was simulated using the steady-state coverage profiles as the initial condition for the model and zero coverage at $z = 0$ as the feed boundary condition. The retentate flux (flux out of the membrane on the feed side as the membrane emptied after a switch to pure He feed) was calculated using the coverage difference between the first and second spatial nodes just as the permeate flux was calculated from the coverage gradient between the last two spatial nodes.

Heat Effects

The above analysis assumed that the zeolite layer was isothermal during the transient measurement. The heat of adsorption, which is small for the gases used, is partially dissipated by forced convective heat transfer to the feedstream, and to a lesser extent by conduction and free convection on the support side. To model the heat transfer, the support-side heat loss was neglected, and the zeolite was assumed to be of uniform temperature T to obtain the energy balance

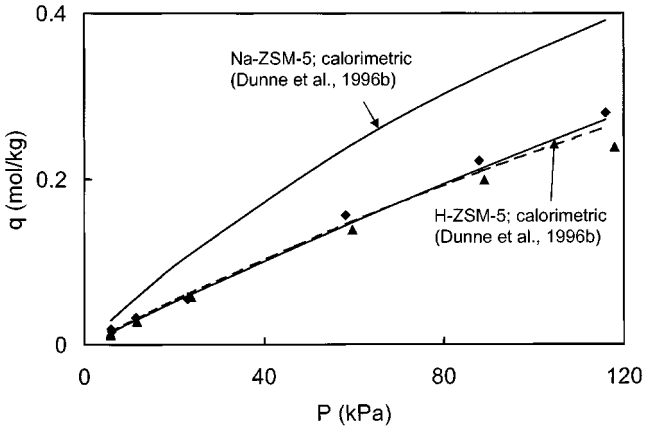

Figure 3. Adsorption isotherms for N_2.

▲ = Data from M1; ♦ = data from M2; dashed line = model fit; solid line = isotherm from literature.

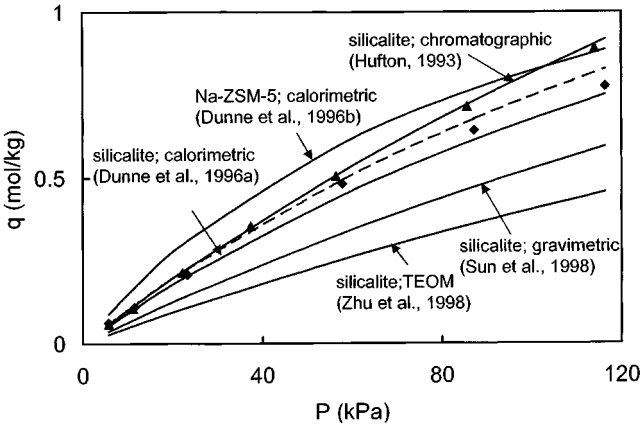

Figure 4. Adsorption isotherms for CH_4.

▲ = Data from M1; ♦ = data from M2; dashed line = model fit; solid line = isotherm from literature.

$$\Delta H_{ads} A(J_{in} - J_{out}) = \rho C_p V \frac{\partial T}{\partial t} + hA(T - T_\infty) \quad (18)$$

where ΔH_{ads} (kJ/mol) is the heat of adsorption, C_p (kJ/kg K) is the heat capacity of the zeolite, V is the volume of the zeolite ($A\delta$, m^3), h (kJ/m^2/s/K) is the convective heat-transfer coefficient of the feed gas, and T_∞ (K) is the feed temperature. Equation 18 was solved for the temperature as a function of time

$$T(t) = \exp(-at) \cdot \int_o^t \phi(t') \cdot \exp(at')dt' + T_\infty \quad (19)$$

where the heat generation as a function of time is

$$\phi(t) = \frac{\Delta H_{ads}}{\rho C_p \delta}(J_{in} - J_{out}) \quad (20)$$

and a (L/s) is a constant defined by

$$a = \frac{h}{\rho C_p \delta} \quad (21)$$

Results

Although the membranes were not analyzed by SEM, images of membranes prepared in the same manner but with only one crystallization layer showing a zeolite layer approximately 110 μm thick on top of the support. Since the membranes used in this study were prepared with three crystallization layers, they are likely to be greater than 110 μm thick. Additionally, the thickness determined from SEM does not include zeolite crystals embedded in the support. Since the synthesis procedure for these membranes allowed the gel to soak into the support before crystallization, the effective thicknesses are probably higher than that measured by SEM.

Isotherms for N_2, CH_4, and CO_2 generated at 298 K using the method described above are compared to isotherms from

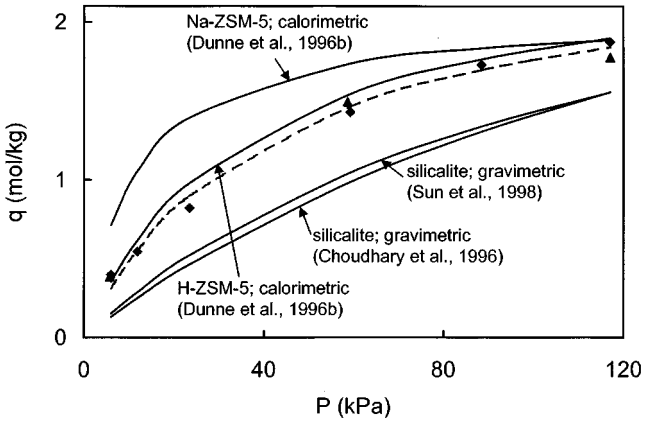

Figure 5. Adsorption isotherms for CO_2.

▲ = data from M1; ♦ = data from M2; dashed line = model fit; solid line = isotherm from literature.

the literature in Figures 3–5. The agreement is excellent with isotherms reported for zeolite crystals. The amounts adsorbed in the membrane at steady state were determined from the transients (Q_t). Equation 17 was minimized for the 34 transient experiments represented as points on the isotherms to determine the 8 parameters: q_{sat} and b for the three gases and the two membrane thicknesses. The dashed lines on the isotherms represent the best fits of the calculated adsorption amounts (Q_c) from this minimization, and thus describe the adsorption properties of both membranes. For all three gases, the Q_t values were higher for membrane M2 than M1 indicating that M2 is thicker. The adsorption parameters determined from this analysis are in Table 1; parameters from other measurement techniques on zeolite crystals are included for comparison. The membrane thicknesses determined from the least-squares regression of $(Q_c - Q_t)^2$ were 220 and 250 μm for M1 and M2, respectively.

Although the adsorption properties were assumed to be the same for both membranes, the diffusion properties were not. Nonidealities in the structure, such as surface barriers and nonzeolite pores in parallel and in series with zeolite pores, are more likely to affect diffusion than adsorptive properties. The adsorption parameters and membrane thicknesses were used in Eq. 10 to calculate Maxwell-Stefan diffusion coefficients from the steady-state fluxes. The calculated $Đ_{MS}$ values are shown in Figure 6. The Maxwell-Stefan diffusion coefficients increased slightly for feed partial pressures between 5 and 120 kPa for all three gases through both membranes. If the Darken approximation is correct, $Đ_{MS}$ should be independent of feed partial pressure. Since $Đ_{MS}$ was assumed to be constant in the model, the relationship between $Đ_{MS}$ and partial pressure (or coverage) cannot be deduced directly from Figure 6, although $Đ_{MS}$ increases with pressure.

The diffusion coefficients are in the 10^{-10} m^2/s range; this agrees with some macroscopic measurements, but is up to two orders of magnitude lower than those measured by microscopic methods (Table 2). The CO_2 and CH_4 diffusion coefficients were comparable between the two membranes, whereas those for N_2 were approximately 30–40% higher for membrane M2.

Figures 7–9 show typical transient approaches to steady state for N_2, CH_4, and CO_2 through these H-ZSM-5 membranes at 298 K for a range of feed pressures. The model is forced to match the steady-state flux value because the diffusion coefficients were calculated from the steady-state flux. The agreement between the model and the measured transients is good for all three gases, although the prediction is somewhat better for N_2 than for CH_4 and CO_2. The model predicts a shorter breakthrough time and more shallow slope of the rise to steady state for CH_4 and CO_2 than is seen experimentally. Transient responses when the feed gas was replaced with helium after steady state had been attained are shown in Figures 10–12. The model tends to predict the decay in flux well for lower initial feed partial pressures, but, for higher coverage conditions, the model predicts a steeper drop from steady state than is measured.

The zeolite membrane temperature increase during the transient was estimated using Eqs. 19–21 and the modeled J_{in} and J_{out} for all measurement conditions used. Heats of adsorption for N_2, CH_4, and CO_2 are 20.7, 26.5, and 38.0 kJ/mol, respectively (Dunne et al., 1996a,b). The feedstream heat-transfer coefficient was estimated as 0.1 kJ/m^2 s K (Bird et al., 1960). The zeolite heat capacity was assumed to be 3.8 kJ/kg K, as calculated for H-mordenite zeolites (Mohamed, 2001). The largest estimated temperature rise was 3.9 K, which was for CO_2 (highest heat of adsorption and most mols adsorbed) with 100% feed. The maximum temperature rises

Table 1. Adsorption Isotherm Parameters

Gas	q_{sat}(mol/kg)	$b \times 10^3$ (kPa^{-1})	Ref.
N_2	1.4	2.0	this study
	2.52	1.0	H-ZSM-5, calorimetric (Dunne et al., 1996b)
	1.13	4.6	Na-ZSM-5, calorimetric (Dunne et al., 1996b)
CH_4	2.5	4.2	this study
	1.65	10	Na-ZSM-5, calorimetric (Dunne et al., 1996b)
	3.84	2.7	silicalite, chromatographic (Hufton and Danner, 1993)
	2.28	4.2	silicalite, calorimetric (Dunne et al., 1996a)
	2.68	2.5	silicalite, gravimetric (Sun et al., 1998)
	2.24	2.2	silicalite, TEOM (Zhu et al., 1998)
CO_2	2.5	24	this study
	2.48	28	H-ZSM-5, calorimetric (Dunne et al., 1996b)
	2.07	88	Na-ZSM-4, calorimetric (Dunne et al., 1996b)
	3.81	5.9	silicalite, gravimetric (Choudhary and Mayadevi, 1996)
	3.09	8.7	silicate, gravimetric (Sun et al., 1998)

Table 2. Corrected Diffusion Coefficients for CH_4 through Silicalite or ZSM-5 at around 300 K*

$Đ_{MS}$ ($\times 10^{-10}$ m^2/s)	Method	Ref.
5	Membrane	This study
8	Single crystal membrane	Sun et al., 1996
27–32	Membrane	Kapteijn et al., 1995b
1.1	Membrane	Hayhurst and Paravar, 1988
150	MD	Maginn et al., 1993
30–140	MD	Goodbody et al., 1991
36	MD	Catlow et al., 1991
38	PFNMR	Datema et al., 1991
92	PFNMR	Caro et al., 1985
50	QENS	Jobic et al., 1989
20	Chromatography	Hufton and Danner, 1993

*Adapted from Kapteijn et al. (1995b).

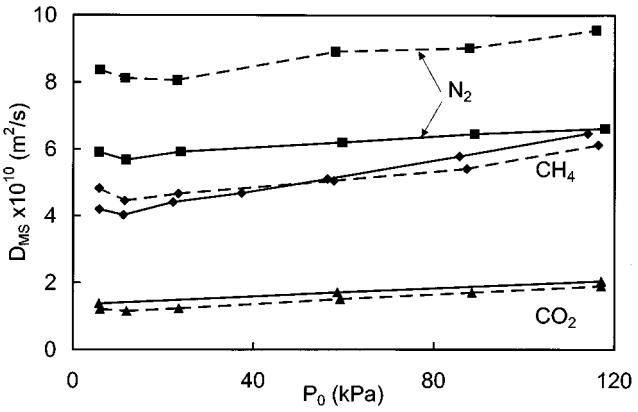

Figure 6. $Đ_{MS}$ values calculated by Eq. 12 as function of feed partial pressure for N_2 (■), CH_4 (♦), and CO_2 (▲) through M1 (solid lines) and M2 (dashed lines).

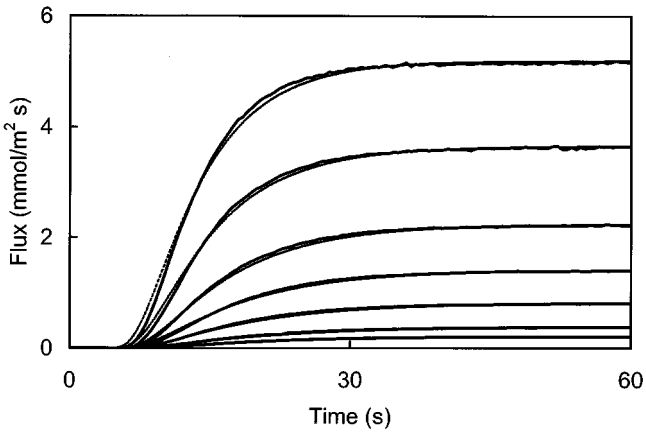

Figure 8. Transient permeate rise response for step change in feed from He to CH_4 (P_0 = 6, 11, 22, 37, 56, 86, 114 kPa).

Solid line = experimental data; dashed line = Maxwell-Stefan model.

estimated for N_2 and CH_4 were 0.4 and 1.4 K. The temperature rises are expected to be lower than these values, and no temperature increase was observed for the gas streams during the transient experiments. The q_{sat} is a weak function of temperature (Zhu et al., 1998), so it would not be affected significantly by these temperature rises. The adsorption equi-

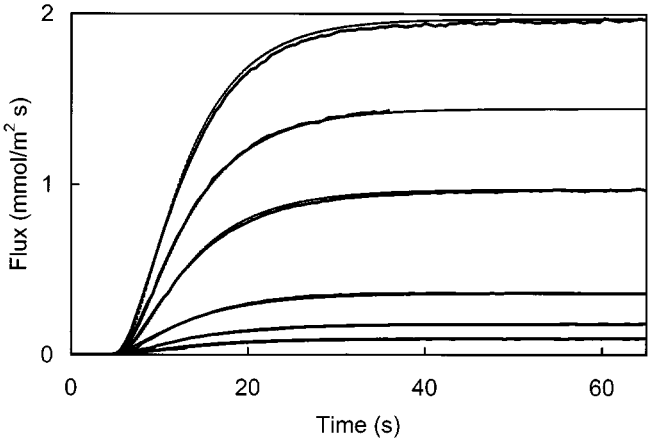

Figure 7. Transient permeate rise response for step change in feed from He to N_2 (P_0 = 6, 11, 23, 58, 88, 116 kPa).

Solid line = experimental data; dashed line = Maxwell-Stefan model.

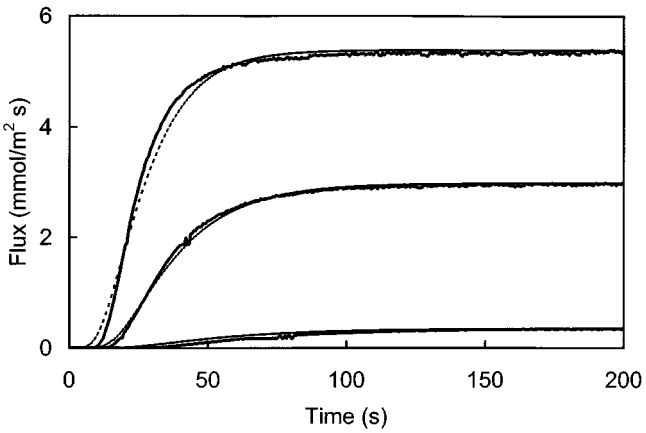

Figure 9. Transient permeate rise response for step change in feed from He to CO_2 (P_0 = 6, 59, 117 kPa).

Solid line = experimental data; dashed line = Maxwell-Stefan model.

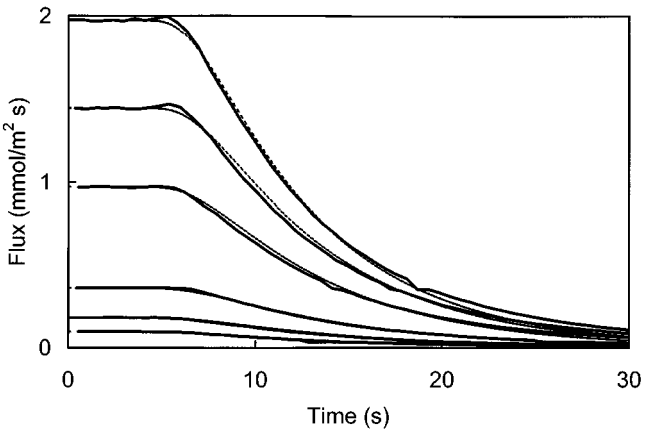

Figure 10. Transient permeate drop response for step change in feed from N_2 to He.

Solid line = experimental data; dashed line = Maxwell-Stefan model.

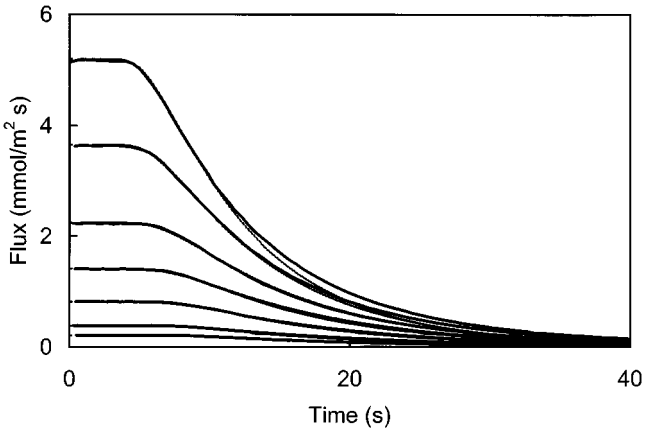

Figure 11. Transient permeate drop response for step change in feed from CH_4 to He.

Solid line = experimental data; dashed line = Maxwell-Stefan model.

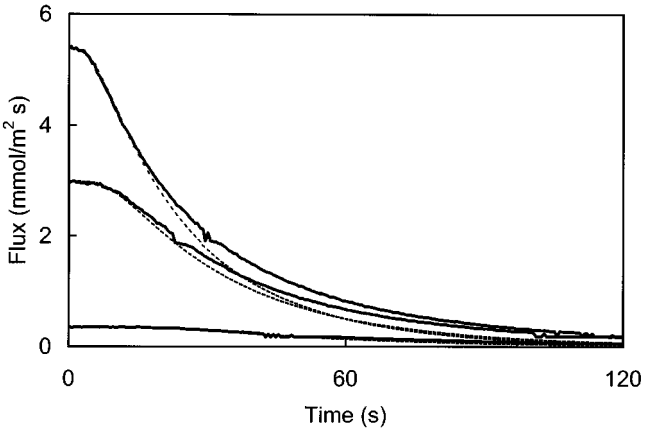

Figure 12. Transient permeate drop response for step change in feed from CO_2 to He.

Solid line = experimental data; dashed line = Maxwell-Stefan model.

librium constant b increases exponentially with temperature, so it would be more in error, but that error would be less than 20% of its value, even for CO_2.

Discussion

The approach outlined for measuring zeolite membrane adsorption and diffusion properties from transport measurements is based on the assumptions that the flow is through zeolite pores and that crystals that adsorb permeating gases are part of the transport pathways. If permeating gases adsorb in crystals that are not part of the membrane pathways, the coverages will be overestimated. The parameters determined by this technique are only meaningful if the membranes studied are of high quality with zeolite pores dominating the transport. Membranes M1 and M2 had n-C_4/i-C_4 ideal selectivities at 298 K of 30–32, which are similar to or higher than butane ideal selectivities reported in the literature for MFI-type zeolite membranes at 300 K (Nishiyama et al., 2001). The transient response of n-C_4 at 373 K also indicates that the membranes were of high quality with the majority of the flow through zeolite pores. Burggraaf et al. (1998) measured the transient response of n-C_4 at 373 K through silicalite membranes with a mass spectrometer. Their n-C_4 transient approached steady state in two distinct stages. One breakthrough was at 13 s, and it plateaued until another breakthrough at 21 s. They attributed the first breakthrough to flow through parallel nonzeolite pores with a shorter transport time and concluded that their membrane was relatively defect-free, because the steady-state flux (zeolite plus nonzeolite pores) was five orders of magnitude higher than the first plateau. Transient n-C_4 fluxes through membranes M1 and M2 at 373 K show a similar breakthrough after approximately 20 s (Figure 13), but any plateau at a shorter time could not be distinguished from the background signal. Since the limit of detection was five orders of magnitude lower than the steady-state flux, this leads to the conclusion that less than 0.001% of the flow through these H-ZSM-5 membranes is through parallel pathways with shorter transients. Thus, these membranes can be modeled as having all flow through zeolite pores.

Adsorption Isotherms

As shown in Figures 3 and 5, the calculated N_2 and CO_2 isotherms are almost identical to those reported by Dunne et al. (1996b) for H-ZSM-5. An isotherm for CH_4 in H-ZSM-5 was not found in the literature, but the calculated isotherm in Figure 4 is between the Na-ZSM-5 and silicalite isotherms reported from calorimetric studies. For a given pressure, the coverage tends to increase with sorbate in the order, silicalite < H-ZSM-5 < Na-ZSM-5, for these light gases in the pressure range studied, and the CH_4 isotherm calculated from the transient measurements follows this trend. Both the CH_4 and CO_2 isotherms on silicalite have wide ranges of coverage values in the literature. The reported coverages on silicalite in the 0 to 120 kPa range increased with measurement method in the order TEOM < gravimetric < calorimetric < chromatographic. The two CO_2 isotherms on silicalite that were determined gravimetrically were comparable although

measured by different groups, suggesting that the variances seen for isotherms are likely due to the measurement method.

The range of pressures where the isotherm is measured can greatly influence the values of the parameters. The results in Figures 3–5 are for low coverages. Under these conditions, b can be estimated with greater accuracy than can q_{sat}, which is better estimated from measurements at high coverages. Sun et al. (1998) measured isotherms at pressures up to 2,000 kPa, and those by Zhu et al. (1998) were up to 500 kPa, whereas the rest of the isotherms in Figures 3–5 were measured below 200 kPa. In general, isotherms from measurements at higher pressures have lower q_{sat} values. Thus, q_{sat} values measured at low coverages should be considered upper limits. Additionally, parameter values can be highly sensitive to the analysis method. The N_2 isotherm measured by the membrane transient method falls almost directly on top of the isotherm reported by Dunne et al. for H-ZSM-5 powders measured calorimetrically, but the Langmuir parameters are significantly different. The q_{sat} value from the transient method is about half of that obtained for the powder and the adsorption equilibrium constant (b) is twice as high. Similarly, the two CO_2 isotherms determined gravimetrically are similar to each other in the pressure range reported, but have q_{sat} and b parameters differing by approximately 20% and 30%, respectively.

The isotherms obtained for the membranes are quite similar to isotherms measured calorimetrically for H-ZSM-5 powders. This is a strong indication that the transient membrane measurement method used to obtain the isotherms is valid and at least as accurate as methods that have been used on zeolite crystals. Since the model assumes the polycrystalline zeolite film is a single crystal, the similarities of the isotherms are remarkable and provide a strong argument that zeolite membranes and zeolite powders have comparable adsorption properties. The isotherm similarity is also a direct indication that transport of these light gases takes place through zeolite pores, and that the fraction of adsorbing molecules that do not participate in transport is small.

Membrane Thickness

The measured number of mols at steady state (Q_t) was higher in membrane M2 than M1 for all *three* gases, indicating that M2 is thicker. Even though M2 was thicker according to this measurement, the N_2 flux was higher through membrane M2 than M1. Methane and CO_2 steady-state fluxes were higher through M1 than M2, as would be expected. The ratio of Q_t for membrane M2 over that for M1 averaged over all conditions and gases studied was 1.2 ± 0.1, indicating that M2 is 10–30% thicker than M1. The thicknesses of membranes M1 and M2 calculated from the transients were 220 and 250 μm, respectively. These membranes were synthesized with three crystallization layers. A membrane with two layers synthesized in the same manner had a thickness of approximately 110 μm by SEM imaging. Thus, estimates of 220–250 μm for these membranes may be slightly high, but are the correct order of magnitude.

Because of the model assumptions, the estimated membrane thickness corresponds to that of a single solid slab with a sorption capacity equivalent to that of the membrane. Zeolite crystals inside the support will contribute to the measured Q_t, and thus increase the effective thickness. Also, if the support provides a resistance to mass transfer or reduces the mixing on the permeate side such that the coverage at $z = \delta$ is greater than that assumed based on the concentration of permeant in the permeate gas flow, the effective thickness will be overestimated. If the steady-state coverage at the permeate boundary is higher than that calculated by P_δ (which is based on the concentration of permeant in the permeate), the coverage will be higher at the higher z values and the membrane would not need to be as thick to contain the same number of mols. The effect of the sweep gas has also not been taken into consideration in the model. Back diffusing helium would tend to slow down the permeating molecules, thereby increasing the effective thickness measured by a transport method.

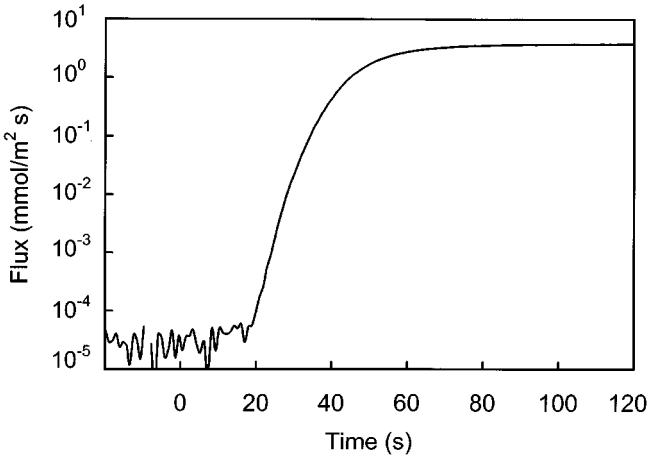

Figure 13. Transient permeate rise response for step change in feed from He to *n*-C_4 at 373 K through M1.

Diffusion Coefficients

The diffusion coefficients of CO_2 and CH_4 were nearly the same for membranes M1 and M2, but the diffusion coefficient of N_2 for membrane M2 was almost 50% higher than for M1. Since the diffusion coefficients for CH_4 and CO_2 are essentially the same for the two membranes, the structures of the membranes are similar. Nonzeolite pores or surface barriers are likely to affect N_2, CH_4, and CO_2 permeation in a similar manner, so the discrepancies in the diffusion coefficients for N_2 are most likely due to inaccuracies in the measurements.

The $Đ_{MS}$ values in Figure 6 are the same order of magnitude as those determined in the transient measurements at low pressure (up to 7 kPa) by Sun et al. (1996) for a single crystal membrane. They modeled the intracrystalline diffusion as Fickian with a constant diffusion coefficient. They applied the Darken correction factor and calculated corrected diffusion coefficients for CO_2 and C_1-C_4 alkanes in the 10^{-10} m^2/s range. Since the diffusion coefficients through the polycrystalline membranes are similar to their measurements for single crystals, flow through zeolite pores apparently dominates the transport through the polycrystalline membranes,

and surface barriers and nonzeolite pores do not significantly affect the diffusion.

Table 2 shows CH_4 diffusion coefficients from the current study compared to those from macroscopic and microscopic techniques. The diffusion coefficients range over three orders of magnitude, with those determined from transport methods (chromatography, FR, uptake, membrane) generally being lower than those from molecular dynamics (MD) or spectroscopic measurements. Spectroscopic and MD methods yield self diffusion coefficients by measuring movements of molecules on a nanometer to micrometer scale, and are equilibrium based, whereas transport methods measure movement through crystals, beds of crystals, or polycrystalline films and operate under nonequilibrium conditions. In packed beds and films, surface barriers can inhibit diffusion and lower measured diffusion coefficients. Another possible reason for the discrepancy between diffusion coefficients measured by microscopic and macroscopic methods is that some assumptions in the models used in calculating diffusion coefficients from transport (macroscopic) techniques may be invalid (Kapteijn et al., 1995b). Finally, microscopic methods are most accurate for fast diffusion processes ($D > 10^{-8}$ m^2/s), whereas macroscopic methods are most accurate for slower processes ($D < 10^{-9}$ m^2/s), so diffusion through zeolites, which is often close to the limits of these ranges, is more difficult to measure accurately by either method (Sun et al., 1996).

Kapteijn et al. (1995b) used the Maxwell-Stefan formulation for diffusion at steady state to obtain diffusion coefficients of light alkanes through silicalite. Their CH_4 diffusion coefficients through silicalite are 5–6 times higher than the $Đ_{MS}$ measured for CH_4 through our H-ZSM-5 membranes. Part of this discrepancy may result because their membrane was silicalite and ours are H-ZSM-5. Bakker et al. (1997) observed that diffusion coefficients for a silicalite-1 membrane decreased with increasing heat of adsorption for noble gases (He, Ne, Ar, Kr, Xe), inorganic gases (H_2, N_2, CO, CO_2, SF_6), and alkanes (CH_4, C_2H_6, C_3H_8, n-C_4, i-C_4) (Figure 14). Since the heats of adsorption are higher on ZSM-5 than on silicalite (Dunne et al., 1996a,b), diffusion coefficients through ZSM-5 may be lower than through silicalite. Diffusion coefficients also vary over a wide range so the difference may be due to the accuracy of making such measurements.

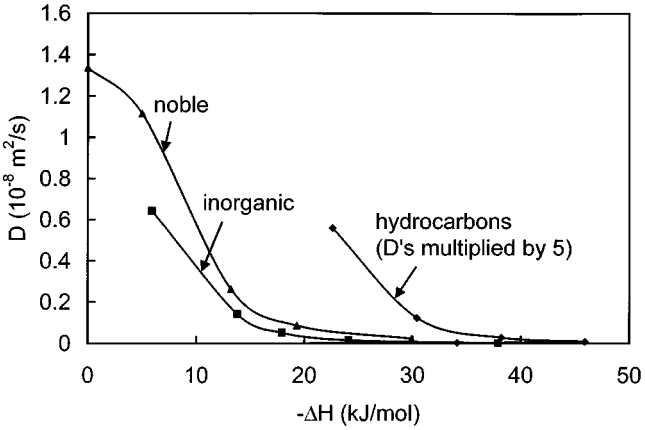

Figure 14. Surface diffusion coefficient dependence on heat of adsorption for noble gases (He, Ne, Ar, Kr, Xe), inorganic gases (H_2, N_2, CO, CO_2, SF_6), and hydrocarbons (CH_4, C_2H_6, C_3H_8, n-C_4, i-C_4).

Adapted from Bakker et al. (1997).

Concentration Dependence of $Đ_{MS}$

Maxwell-Stefan diffusion coefficients determined from the steady-state fluxes were higher for higher feed partial pressures, indicating that $Đ_{MS}$ is a function of concentration. Single file diffusion of one component through zeolite membranes modeled by the Maxwell-Stefan equation applies the Darken approximation, which assumes $Đ_{MS}$ is independent of coverage. However, previous studies have also shown that the Darken approximation does not always hold and $Đ_{MS}$ may vary with coverage (Jobic et al., 1999; Kapteijn et al., 1995b; Skoulidas and Sholl, 2001). Kapteijn et al. (1995b) found that $Đ_{MS}$ increased by up to a factor of 3 from $P_o = 20$ to 100 kPa for light alkanes and alkenes through silicalite. Skoulidas et al. used molecular simulations to model the permeation of CH_4 and CF_4 through silicalite and found that $Đ_{MS}$ decreased with coverage (Skoulidas and Sholl, 2001). Jobic et al. measured the transport and self-diffusivities of D_2 in NaX simultaneously by quasi-elastic neutron scattering (QENS), calculated the corrected diffusion coefficient assuming the Darken approximation, and found that the corrected diffusion coefficient (or $Đ_{MS}$ for single file diffusion) increased with coverage up to a certain loading where it leveled off (Jobic et al., 1999).

Possible physical explanations for why $Đ_{MS}$ might depend on coverage include interactions of molecules with each other in the zeolite structure and sorption of more than one molecule per sorption site. Xiao and Wei investigated the concentration dependence of Fickian diffusion coefficient experimentally under various temperature and loading conditions and developed a model including effects of molecule-molecule interactions within the zeolite. For sufficiently high loadings of benzene, toluene, and 2-methylbutane in ZSM-5 (> 4 molecules/unit cell), the diffusion coefficient increased more sharply with occupancy than with the $1/(1-\theta)$ dependence assumption, which was consistent with a lattice model involving soft repulsion between molecules (Xiao and Wei, 1992). Conditions permitting molecules inside the zeolite cages to interact could thus lead to $Đ_{MS}$ values that increase with coverage.

Since each $Đ_{MS}$ point shown in Figure 6 was calculated based on a transient that assumed $Đ_{MS}$ was independent of coverage, the functionality of $Đ_{MS}$ with loading cannot be determined directly from these plots. However, assuming a function for $Đ_{MS}$ and modifying the model to include this dependence could improve the model.

Transient Model Fits

The Maxwell-Stefan model fits the transient responses for both positive and negative step changes in N_2, CH_4, and CO_2 feed fairly well, and in general the model predicts the measured responses better when the coverages are lower. That is, the fits are better for lower feed partial pressures, and they are better for N_2 than CH_4 or CO_2 because N_2 has a lower

heat of adsorption. Deviations may be due to problems in the measurements or assumptions that are less valid at higher coverages. For example, if $Đ_{MS}$ increases with coverage, the assumption of constant $Đ_{MS}$ will be less valid when the coverage gradient is higher. Since the downstream coverage is always low due to the sweep gas, the coverage gradients increase with increasing feed partial pressure and with increasing adsorption strength ($CO_2 > CH_4 > N_2$). Therefore, the model with constant $Đ_{MS}$ should fit better when coverages are lower, as is observed. A mass-transfer resistance on the support side may also affect the fits. If the sweep gas does not remove the desorbing gas on the permeate side efficiently, the coverage at the permeate boundary would be higher than predicted by the model, and thus the gradient would be less across the membrane. At higher feed coverages, the fluxes are higher and the partial pressure of permeant in the support is higher; this leads to larger deviations between the modeled and measured coverage at the permeate boundary.

Conclusions

- A method was developed to measure adsorption isotherms of zeolite membranes from transient response measurements. The effective membrane thicknesses are also estimated nondestructively. This method characterizes the pathways involved in transport through the membrane rather than characterizing the bulk of the zeolite film.
- Adsorption isotherms determined from transport measurements of N_2, CH_4, and CO_2 on H-ZSM-5 membranes at 298 K are remarkably similar to adsorption isotherms measured for ZSM-5 crystals by calorimetry.
- Maxwell-Stefan diffusion coefficients determined from transient analysis are of the same order of magnitude as those measured by other macroscopic techniques. This indicates that transport through these zeolite membranes occurs mainly through zeolite pores. Butane transients at 373 K indicate that less than 0.001% of the flow through these membranes is through parallel nonzeolite pores with shorter path lengths
- Maxwell-Stefan diffusion coefficients increase slightly with increasing feed partial pressure, indicating that they depend on concentration and that the Darken approximation does not completely model diffusion of light gases through ZSM-5 membranes.

Acknowledgments

We gratefully acknowledge support by the National Science Foundation Grant CTS-9908796. We gratefully acknowledge Dr. Kazuhiro Tanaka of Yamiguchi University for his design and original setup of the experimental apparatus used in this research and Professor David S. Sholl of Carnegie Mellon University for his suggestions on the modeling.

Literature Cited

Bai, C., M.-D. Jia, J. L. Falconer, and R. D. Noble, "Preparation and Separation Properties of Silicalite Composite Membranes," *J. Memb. Sci.*, **105**, 79 (1995).

Bakker, W. J. W., F. Kapteijn, J. Poppe, and J. A. Moulijn, "Permeation Characteristics of a Metal-Supported Silicalite-1 Zeolite Membrane," *J. Memb. Sci.*, **117**, 57 (1996).

Bakker, W. J. W., L. J. P. van den Broeke, F. Kapteijn, and J. A. Moulijn, "Temperature Dependence of One-Component Permeation through a Silicalite-1 Membrane," *AIChE J.*, **43**, 2203 (1997).

Bakker, W. J. W., G. Zheng, F. Kapteijn, M. Makkee, and J. A. Moulijn, "Single and Multi-Component Transport through Metal-Supported MFI Zeolite Membranes," *Precision Proc. Tech.*, 425 (1993).

Barrer, R. M., "Porous Crystal Membranes," *J. Chem. Soc., Farad. Trans.*, **86**, 1123 (1990).

Bein, T., "Synthesis and Applications of Molecular Sieve Layers and Membranes," *Chem. Mater.*, **8**, 1636 (1996).

Bird, R. B., W. E. Stewart, and E. N. Lightfoot, *Transport Phenomena*, Wiley, New York (1960).

Bulow, M., H. Schlodder, L. V. C. Rees, and R. E. Richards, *7th Proc. Int. Conf. Zeolites*, Tokyo, 579 (1986).

Burggraaf, A. J., Z. A. E. P. Vroon, K. Keizer, and H. Verweij, "Permeation of Single Gases in Thin Zeolite MFI Membranes," *J. Memb. Sci.*, **144**, 77 (1998).

Caro, J., M. Bulow, W. Schirmer, J. Kerger, W. Heink, H. Pfeifer, and S. P. Zdanov, "Microdynamics of Methane, Ethane, and Propane in ZSM-5-Type Zeolites," *J. Chem. Soc., Farad. Trans.*, **81**, 2541 (1985).

Catlow, C. R. A., C. M. Freeman, B. Vessal, S. M. Tomlinson, and M. Leslie, "Molecular-Dynamics Studies of Hydrocarbon Diffusion in Zeolites," *J. Chem. Soc., Farad. Trans.*, **87**, 1947 (1991).

Choudhary, V. R., and S. Mayadevi, "Adsorption of Methane, Ethane, Ethylene, and Carbon Dioxide on Silicalite-I, *Zeolites*, **17**, 501 (1996).

Datema, K. P., C. J. J. d. Ouden, W. D. Yistra, H. P. C. E. Kuipers, M. F. M. Post, and J. Karger, "Fourier-Transform Pulsed-Field-Gradient H-1 Nuclear-Magnetic-Resonance Investigation of the Diffusion of Light Normal-Alkanes in Zeolite ZSM-5," *J. Chem. Soc., Farad. Trans.*, **87**, 1935 (1991).

Davis, M. E., and R. F. Lobo, "Zeolite and Molecular Sieve Synthesis," *Chem. Mater.*, **4**, 756 (1992).

den Exter, M. J., J. C. Jansen, J. M. van de Graaf, F. Kapteijn, J. A. Moulijn, and H. van Bekkum, "Zeolite-Based Membranes Preparation, Performance and Prospects," *Stud. Surf. Sci. Catal.; Rec. Adv. New Horizons in Zeolite Sci. and Tech.*, **102**, 413 (1996).

Dunne, J. A., R. Mariwala, M. Rao, S. Sircar, R. J. Gorte, and A. L. Myers, "Calorimetric Heats of Adsorption and Adsorption Isotherms. 1. O_2, N_2, Ar, CO_2, CH_4, C_2H_6, and SF_6 on Silicalite," *Langmuir*, **12**, 5888 (1996a).

Dunne, J. A., M. Rao, S. Sircar, R. J. Gorte, and A. L. Myers, "Calorimetric Heats of Adsorption and Adsorption Isotherms. 2. O_2, N_2, Ar, CO_2, CH_4, C_2H_6, and SF_6 on NaX, H-ZSM-5, and Na-ZSM-5 Zeolites," *Langmuir*, **12**, 5896 (1996b).

Gardner, T. Q., J. L. Falconer, R. D. Noble and M. Zieverink, "Analysis of Transient Permeation Fluxes into and out of Membranes for Adsorption Measurements," *Chem. Eng. Sci.*, in press (2002).

Goodbody, S. J., K. Watanabe, D. MacGowan, J. P. R. B. Walton, and N. Quirke, "Molecular Simulation of Methane and Butane in Silicalite," *J. Chem. Soc., Farad. Trans.*, **87**, 1951 (1991).

Gora, L., N. Nishiyama, J. C. Jansen, F. Kapteijn, V. Teplyakov, and T. Maschmeyer, "Highly Reproducible High-Flux Silicalite-1 Membranes: Optimization of Silicalite-1 Membrane Preparation," *Sep. & Purif. Tech.*, **22-3**, 223 (2001).

Hayhurst, D. T., and A. Paravar, "Diffusion of C_1 to C_5 Normal Paraffins in Silicalite," *Zeolites*, **8**, 27 (1988).

Hedlund, J., B. Schoeman, and J. Sterte, "Ultrathin Oriented Zeolite LTA Films," *Chem. Commun.*, **13**, 1193 (1997).

Hufton, J. R., and R. P. Danner, "Chromatographic Studies of Alkanes in Silicalite: Equilibrium Properties," *AIChE J.*, **39**, 954 (1993).

Hufton, J. R., and R. P. Danner, "Chromatographic Study of Alkanes in Silicalite: Transport Properties," *AIChE J.*, **39**, 962 (1993).

Jia, M.-D., B. Chen, R. D. Noble, and J. L. Falconer, "Ceramic-Zeolite Composite Membranes and their Application for Separation of Vapor/Gas Mixtures," *J. Memb. Sci.*, **90**, 1 (1994).

Jobic, H., M. Bee, and J. Caro, "Translational and Rotational-Dynamics of Methane in ZSM-5 Zeolite—A Quasi-Elastic Neutron-Scattering Study," *Zeolites*, **9**, 312 (1989).

Jobic, H., J. Karger, and M. Bee, "Simultaneous Measurement of Self- and Transport Diffusivities in Zeolites," *Phys. Rev. Lett.*, **82**, 4260 (1999).
June, R. L., A. T. Bell, and D. N. Theodorou, "Molecular Dynamics Studies of Butane and Hexane in Silicalite," *J. Phys. Chem.*, **96**, 1051 (1992).
June, R. L., A. T. Bell, and D. N. Theodorou, "Prediction of Low Occupancy Sorption of Alkanes in Silicalite," *J. Phys. Chem.*, **94**, 1508 (1990).
Kapteijn, F., W. J. W. Bakker, J. M. van de Graaf, G. Zheng, J. Poppe, and J. A. Moulijn, "Permeation and Separation Behavior of a Silicalite-1 Membrane," *Catal. Today*, **25**, 213 (1995a).
Kapteijn, F., W. J. W. Bakker, G. Zheng, J. Poppe, and J. A. Moulijn, "Permeation and Separation of Light Hydrocarbons through a Silicalite-1 Membrane—Application of the Generalized Maxwell-Stefan Equations," *Chem. Eng. J.*, **57**, 145 (1995b).
Kosslick, H., V. A. Tuan, R. Fricke, C. Peuker, W. Pilz, and W. Storek, "Synthesis and Characterization of Ge-ZSM-5 zeolites," *J. Phys. Chem.*, **97**, 5678 (1993).
Krishna, R., "A Unified Approach to the Modelling of Intraparticle Diffusion in Adsorption Processes," *Gas Sep. & Purif.*, **7**, 91 (1993).
Krishna, R., and L. J. P. van den Broeke, "The Maxwell-Stefan Description of Mass Transport Across Zeolite Membranes," *The Chem. Eng. J.*, **57**, 155 (1995).
Kusakabe, K., T. Kuroda, and S. Morooka, "Separation of Carbon Dioxide from Nitrogen Using Ion-Exchanged Faujasite-Type Zeolite Membranes Formed on Porous Support Tubes," *J. Memb. Sci.*, **148**, 13 (1998).
Kusakabe, K., T. Kuroda, K. Uchino, Y. Hasegawa, and S. Morooka, "Gas Permeation Properties of Ion-Exchanged Faujasite-Type Zeolite Membranes," *AIChE J.*, **45**, 1220 (1999).
Maginn, E. J., A. T. Bell, and D. N. Theodorou, "Transport Diffusivity of Methane in Silicalite from Equilibrium and Nonequilibrium Simulations," *J. Phys. Chem.*, **97**, 4173 (1993).
Matsukata, M., and E. Kikuchi, "Zeolitic Membranes: Synthesis, Properties, and Prospects," *Bull. Chem. Soc. Jpn.*, **70**, 2341 (1997).
Matsukata, M., N. Nishiyama, and K. Ueyama, "Crystallization of FER and MFI Zeolites by a Vapor-Phase Transport Method," *Microporous Materials*, **7**, 109 (1996).
Matsukata, M., N. Nishiyama, and K. Ueyama, "Synthesis of Zeolites Under Vapor Atmosphere—Effect of Synthetic Conditions on Zeolite Structure," *Microporous Materials*, **1**, 219 (1993).
Mentzen, B. F., "Energetics and Siting of Sorbed Molecules in Zeolites by Computer Simulations. Comparison with Calorimetric and Structural Results: II. *n*-Alkanes in Silicalite," *Materials Res. Bulletin*, **30**, 1333 (1995).
Mohamed, M. M., "Heat Capacities, Phase Transitions and Structural Properties of Cation-Exchanged H-Mordenite Zeolites," *Thermochimica Acta*, **372**, 75 (2001).
Nijhuis, T. A., L. J. P. van den Broeke, M. J. G. Linders, M. Makkee, F. Kapteijn, and J. A. Moulijn, "Modeling of the Transient Sorption and Diffusion Processes in Microporous Materials at Low Pressure," *Catal. Today*, **53**, 189 (1999).
Nishiyama, N., L. Gora, V. Teplyakov, F. Kapteijn, and J. A. Moulijn, "Evaluation of Reproducible High Flux Silicalite-1 Membranes: Gas Permeation and Separation Characterization," *Sep. & Purif. Tech.*, **22-3**, 295 (2001).
Nishiyama, N., T. Matsufuji, K. Ueyama, and M. Matsukata, "FER Membrane Synthesized by a Vapor-Phase Transport Method: its Structure and Separation Characteristics," *Microporous Materials*, **12**, 293 (1997).
Noble, R. D., and J. L. Falconer, "Silicalite-1 Zeolite Composite Membranes," *Catal. Today*, **25**, 209 (1995).
Skoulidas, A. I., and D. S. Sholl, "Direct Tests of the Darken Approximation for Molecular Diffusion in Zeolites Using Equilibrium Molecular Dynamics," *J. Phys. Chem. B*, **105**, 3151 (2001).
Sun, M. S., D. B. Shah, H. H. Xu, and O. Talu, "Adsorption Equilibria of C_1 to C_4 Alkanes, CO_2, and SF_6 on Silicalite," *J. Phys. Chem.*, **102**, 1466 (1998).
Sun, M. S., O. Talu, and D. B. Shah, "Diffusion Measurements through Embedded Zeolite Crystals," *AIChE J.*, **42**, 3001 (1996).
Tuan, V. A., J. L. Falconer, and R. D. Noble, "Alkali-free ZSM-5 Membranes: Preparation Conditions and Separation Performance," *I&EC Res.*, **38**, 3635 (1999).
Tuan, V. A., J. L. Falconer, and R. D. Noble, "Boron Substituted ZSM-5 Membranes: Preparation and Separation Performance," *AIChE J.*, **46**, 1201 (2000).
Tuan, V. A., J. L. Falconer, and R. D. Noble, "Isomorphous Substitution of Al, Fe, B, and Ge into MFI-Zeolite Membranes," *Microporous and Mesoporous Materials*, **41**, 269 (2000).
Tuan, V. A., S. G. Li, R. D. Noble, and J. L. Falconer, "Preparation and Pervaporation Properties of a MEL-Type Zeolite Membrane," *Chem. Commun.*, **6**, 583 (2001).
Xiao, J., and J. Wei, "Diffusion Mechanism of Hydrocarbons in Zeolites: II. Analysis of Experimental Observations," *Chem. Eng. Sci.*, **47**, 1143 (1992).
Xomeritakis, G., A. Gouzmis, S. Nair, T. Okubo, M. He, R. M. Overney, and M. Tsapatsis, "Growth, Microstructure, and Permeation Properties of Supported Zeolite (MFI) Films and Membranes Prepared by Secondary Growth," *Chem. Eng. Sci.*, **54**, 3521 (1999).
Yan, Y., M. E. Davis, and G. R. Gavalas, "Preparation of Zeolite ZSM-5 Membranes by In-Situ Crystallization on Porous α-Al_2O_3," *Ind. Eng. Chem. Res.*, **34**, 1652 (1995).
Zhu, W., J. M. van de Graaf, L. J. P. van den Broeke, F. Kapteijn, and J. A. Moulijn, "TEOM: A Unique Technique for Measuring Adsorption Properties. Light Alkanes in Silicalite-1," *Ind. Eng. Chem. Res.*, **37**, 1934 (1998).

Manuscript received June 29, 2001, and revision received Nov. 21, 2001.